Article

Not peer-reviewed version

Nematicidal Activity and Action Receptor of A Methyl-Accepting Chemotaxis Protein from the Phytopathogen Pseudomonas syringae Against Caenorhabditis elegans

Jiaoqing Li , Haiyan Dai , Anum Bashir , Zhiyong Wang , Yimin An , Xun Yu , Liangzheng Xu * , Lin Li *

Posted Date: 29 August 2023

doi: 10.20944/preprints202308.1827.v1

Keywords: Pseudomonas syringae; methyl-accepting chemotaxis protein; Caenorhabditis elegans; receptor protein; nematicidal activity

Article

Nematicidal Activity and Action Receptor of a Methyl-Accepting Chemotaxis Protein from the Phytopathogen *Pseudomonas syringae* against *Caenorhabditis elegans*

Jiaoqing Li [1,†], Haiyan Dai [2,†], Anum Bashir [2,†], Zhiyong Wang [2], Yimin An [3], Xun Yu [2], Liangzheng Xu [1,*] and Lin Li [2,*]

[1] Guangdong Provincial Key Laboratory of Conservation and Precision Utilization of Characteristic Agricultural Resources in Mountainous Areas, School of Life Sciences, Jiaying University, Meizhou 514015, China; lijiaoqing@jyu.edu.cn (J.L.)

[2] National Key Laboratory of Agricultural Microbiology, College of Life Science and Technology, Huazhong Agricultural University, Wuhan 430070, China; daihaiyan9417@163.com (H.D); anumbashir@webmail.hzau.edu.cn (A.B); wangzhiyong@hbmzu.edu.cn (Z.W.); yuxun@webmail.hzau.edu.cn (X.Y)

[3] Pomelo Engineering Technology Center, School of Life Sciences, Jiaying University, Meizhou 514015, China; anyimin123@sina.com (Y.A.)

* Correspondence: xlzheng@jyu.edu.cn (L.X.); lilin@mail.hzau.edu.cn (L.L.)

† These authors contributed equally to this paper.

Abstract: The conventional phytopathogen *Pseudomonas syringae* has been identified several significant virulence determinants against *Caenorhabditis elegans*, but their mechanisms of action remain elusive. Here, we report the nematicidal activity and action receptor of a methyl-accepting chemotaxis protein (MCP03) of a wild-type *P. syringae* MB03 against *C. elegans*. Purified MCP03 exhibited significant nematicidal toxicity against *C. elegans*, with a half-lethal concentration of 124.4 μg mL^{-1}, and detrimental effects on the growth and brood size of *C. elegans*. Additionally, MCP03-treated worms showed severe pathological destruction of the intestine and ovary, and depressed wrinkles of the cuticle. Through yeast two-hybrid assays, we identified a subunit of a COP9 signalosome, namely CSN-5, functionated as an action receptor of MCP03. *In vitro* pull-down and *in vivo* co-localization assays verified the binding interaction between MCP03 and CSN-5. RNA interference assays confirmed that MCP03 acts on CSN-5 to adversely affect the brood size, growth, and cuticle integrity of *C. elegans*. Following MCP03 infection, the expression of several genes relative to reproduction, growth, and cuticle formation, such as *kgb-1*, *unc-98*, and *col-117*, were significantly downregulated, which implicated the pathological changes of MCP03-treated nematodes. Thus, this study demonstrates that MCP03 acted on the receptor protein CSN-5 causing lethality and detrimental effects on the fertility, growth, and morphogenesis of *C. elegans*, which will provide new insights into the signaling pathways and mechanism underlying the nematicidal action of MCP03 towards *C. elegans*.

Keywords: *Pseudomonas syringae*; methyl-accepting chemotaxis protein; *Caenorhabditis elegans*; receptor protein; nematicidal activity

1. Introduction

Plant-parasitic nematodes (PPNs) are a large group of soil-borne roundworms that primarily attack underground plant parts, leading to stunted growth and endangering nutrient supply from the soil, and causing a first-hand globally annual yielding loss of over $157 billion [1]. These nematodes also increase the susceptibility of plant roots to other pathogenic fungal and bacterial infections and serve as vectors for certain plant-pathogenic viruses [2]. Although various chemical

 doi:10.20944/preprints202308.1827.v1

nematicides and agricultural managements have been the typical implements for controlling PPNs for a long time, integrated biological control has gained increasing incentive as a prioritized approach to combating PPNs due to its sustainability and eco-friendly nature [3,4].

A variety of soil-borne bacteria, mainly belonging to several genera including *Bacillus* [5,6], *Pseudomonas* [7,8], *Pasteuria* [9], and *Burkholderia* [10], etc., have been confirmed the significant nematicidal activity. These bacteria have developed various strategies, such as the production of external toxins, invasive enzymes, or other active substances to trap and kill nematodes; and/or acting as external parasites by utilizing extracellular proteases to digest the nematode cuticle [11]; or producing nematode-toxic metabolites after entering the nematode's body, for instance, the Cry proteins from a nematicidal bacterium *Bacillus thuringiensis* formed lytic pores in the cell membrane of intestinal epithelial cells upon ingestion [12].

Chemotaxis is a conventional behavior by bacteria to sense chemical cues in their surroundings, enabling them to relocate to favorable niches away from toxic substances. The methyl-accepting chemotaxis proteins (MCPs) are a family of chemoreceptors responsible for the chemotactic behaviors of many bacteria [13]. Structurally, MCPs consist of a typical C-terminal cytoplasmic signaling domain (SD), two membrane-spanning helices, and an N-terminal periplasmic ligand-binding domain (LBD). The highly conserved SD domain contains methylated glutamate residues that interact with downstream signaling components, while the less conserved LBD typically contains signal peptide sequences that act as transmembrane segments in mature proteins [14]. Most MCPs also contain a histidine kinases, adenylate cyclases, methyl-accepting proteins, and phosphatases (HAMP) domain that propagates signals from the sensing domain to the cytoplasmic domain [15]. Upon perceiving an external environmental signal, MCP undergoes a conformational change by adopting a hairpin structure, where a series of sensor kinases (such as CheA, CheB, and CheW, etc.) were phosphorylated or self-phosphorylated to stepwise activate the response regulator CheY, which enables phosphorylating the flagellar matrix, resulting in a change in the direction of flagellar rotation [14]. Moreover, chemotaxis is also involved in the pathogenicity of various bacterial pathogens, including *Vibrio cholera* [16], *Coronobacter sakazakii* [17], *Campylobacter jejuni* [18], *Pseudomonas aeruginosa* [18], and *Pseudomonas syringae* [19]. The connection between chemotaxis and pathogenicity relies on the detection of pathogenicity-related signal molecules in the hosts by MCPs, which play a critical role in regulating certain cellular activities, such as biofilm formation, toxin production, exopolysaccharide production, flagellum biosynthesis, cell survival, motility, pathogenicity, and antibiotic resistance [20].

The conventional phytopathogen *P. syringae* has been identified significant nematicidal activity against the model nematode *Caenorhabditis elegans* [21,22], and a recent genome-wide prediction analysis of nematicidal factors in a *P. syringae* wild-type strain MB03 revealed significant nematicidal virulence potential of an MCP (namely MCP03) against *C. elegans* [23]. However, the nematicidal activity and action mechanism of MCP03 remain understudied. In the current study, we investigated the nematicidal activity and action receptor protein of MCP03 for elucidating its pathogenic mechanism. Owing to the current technical limitations of molecular genetic studies on PPNs, *C. elegans* was used as a target nematode due to its well-characterized genetic background [24]. We identified a subunit of a COP9 signalosome (CSN) that served as a receptor protein (namely CSN-5) of MCP03 in *C. elegans*, which associatively exerted destructive effects on the intestinal tract and the ovary, enabled lethal and detrimental effects on the egg-laying, growth, and surface cuticle formation by downregulating the expression of genes relative to these activities. Thus, a putative outline mechanism underlying the nematicidal action of MCP03 following the binding with CSN-5 was proposed.

2. Materials and Methods

2.1. Bacterial and Nematode Strains, Plasmids, and Culture Conditions

Bacterial strains and plasmids used in this study are listed in Supplementary Table S1. Briefly, a wild-type strain of *P. syringae* MB03 [25] (CCTCC No. M2014114, China Center for Type Culture

Preprints (www.preprints.org) | NOT PEER-REVIEWED | Posted: 29 August 2023 doi:10.20944/preprints202308.1827.v1

Collection) provided the gene resource of *mcp03*. *Escherichia coli* strains DH5α, BL21(DE3), and HT115(DE3) were used for cloning, or expression of certain genes using different plasmid vectors, while *E. coli* OP50 cells were used as food for feeding *C. elegans* unless specified. *P. syringae* and *E. coli* cells were routinely cultured at 28 °C and 37 °C in Luria–Bertani (LB) medium [26] supplemented with 100 μg mL^{-1} ampicillin (Amp), or 50 μg mL^{-1} kanamycin (Kan) or 20 μg mL^{-1} tetracycline (Tet) when required, respectively. *C. elegans* strains used in this study include the wild-type Bristol strain N2, the green fluorescence protein (GFP)-labeled transgenic strains FT63 (*dlg*::*gfp*) and LG333 (*skn-1b*::*gfp*) that were obtained from *Caenorhabditis* Genetics Centre (CGC) (College of Biological Sciences, University of Minnesota, MN55108, USA), and the *csn-5* silenced strain by RNAi. All *C. elegans* strains were cultivated at 20 °C under standard conditions on a nematode growth medium (NGM) [22] with *E. coli* OP50 as food. The synchronized worms were prepared following the standard protocol [27].

2.2. Cloning, Expression, Purification, and Labelling of MCP03 Protein

The oligonucleotide primers used in this study are listed in Supplementary Table S1. To construct recombinant plasmid pMB831 [Figure 1A(a)], the *mcp03* gene was amplified by a polymerase chain reaction (PCR) from *P. syringae* MB03 genome (GenBank accession No. NZ_LAGV00000000.1) using the primers F-pET28a-mcp03/ R-pET28a-mcp03. The amplified fragment was inserted into the *Xho* I and *Eco*R I sites of *E. coli* expression vector pET28a to generate pMB831. This recombinant plasmid was then transformed into *E. coli* BL21(DE3) to yield a recombinant strain MB831.

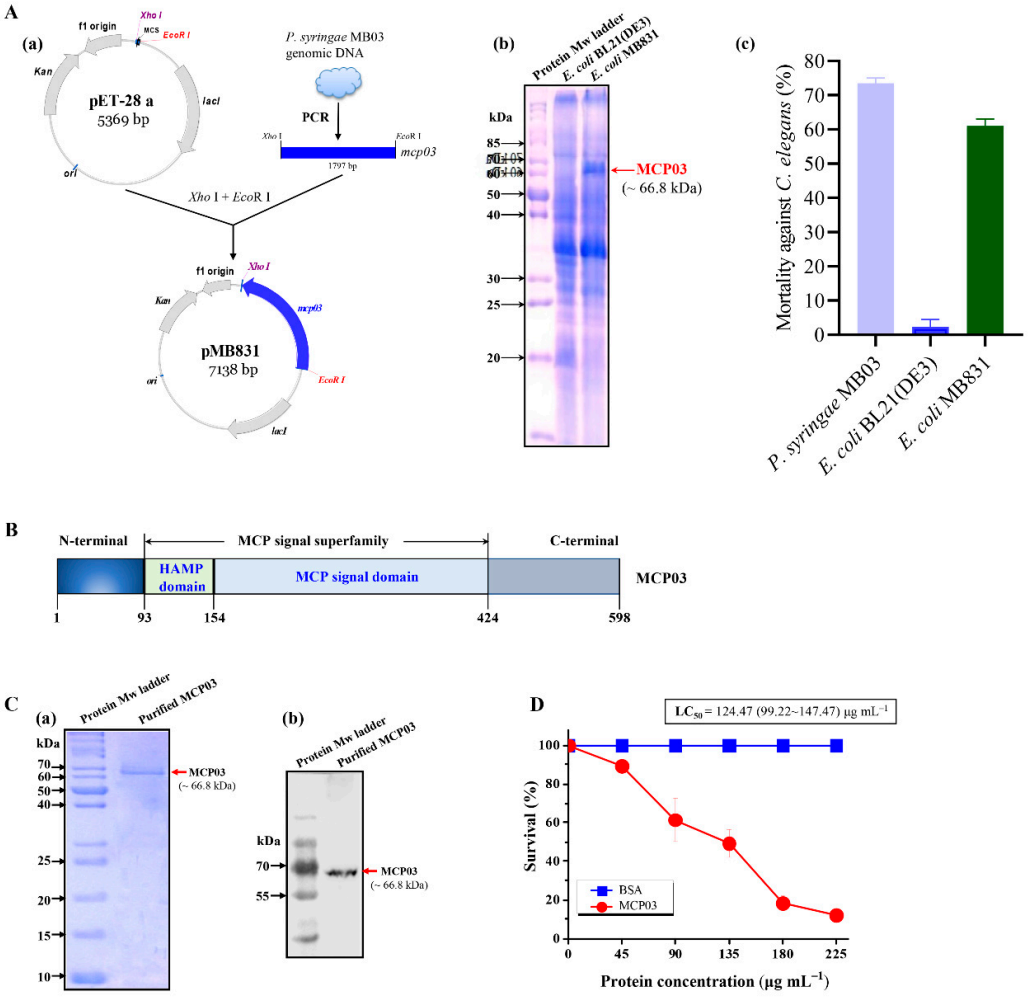

Figure 1. Expression, structural organization, and nematicidal activity of MCP03. In (**A**), (a) Schematic representation of the construction of plasmid pMB831 expressing the *mcp03* gene; (b) SDS-PAGE

 doi:10.20944/preprints202308.1827.v1

analysis of whole-cell lysate of recombinant *E. coli* MB831, *E. coli* BL21(DE3) was used as negative control; (c) Whole-cell nematicidal activity of *E. coli* strain MB831 against *C. elegans*. *P. syringae* MB03 and *E. coli* BL21(DE3) were used as positive and negative control, respectively. In (**B**), Conserved domain analysis of MCP03. In (**C**), SDS-PAGE (a) and Western blot analysis (b) of purified MCP03 protein. (**D**) Nematicidal activity assay of purified MCP03 protein against *C. elegans*. Error bars represent the standard deviations from the mean of three independent experiments.

To induce MCP03 expression, *E. coli* MB831 cells were cultured in LB broth with Kan at 37 °C until a cell optical density at 600 nm (OD_{600}) reached 0.6, then 0.2 mmol L^{-1} isopropyl-*β*-D-thiogalactopyranoside (IPTG) was added to the cultures, which were further incubated at 30 °C for 6 h. The cells were harvested by centrifugation (5000 rpm, 10 min), resuspended in phosphate-buffered saline (PBS, pH 7.4), and were homogenized using a high-pressure homogenizer (NS1001L 2K, Niro Soavi, Germany) at 1000 *psi*. The supernatants were collected by centrifugation (12000 rpm, 10 min, and 4 °C). The MCP03 protein was purified from the supernatants using a nickel nitrilotriacetic acid spin column (Qiagen). The protein samples were then solubilized using 20 mmol L^{-1} HEPES (pH 6.0) and stored at −80 °C after quantification [28]. While acquired, the purified MCP03 was labeled with *N*-hydroxysuccinimide-rhodamine (Rho) (Pierce 46102) according to the previously described protocol [29].

2.3. Nematicidal Bioassay

The nematicidal activity of recombinant *E. coli* intact cells, and the half-lethal concentration (LC_{50}) of purified MCP03 against *C. elegans* was determined using a previously described method [22]. The growth inhibition and brood size assays were performed following previously described procedures [22,30].

2.4. Analysis of C. elegans Intestinal Pathology

The wild-type C. elegans N2 and the transgenic C. elegans FT63(DLG::GFP) were fed with Rho-labeled MCP03 and unlabeled MCP03, respectively, with bovine serum albumin (BSA) as the negative control. The worms were incubated for 72 h and were subjected to fluorescence microscope examination. To facilitate imaging, the worms were rendered unconscious using a 15 mmol L^{-1} sodium azide and then fixed on a microscopic slide coated with 2% agarose. Images of the worms were captured using a fluorescence microscope (80i, Nikon, Japan) in two different modes: green fluorescence (GFP) and red fluorescence (RFP).

2.5. Yeast Two-Hybrid Assay

The yeast two-hybrid (Y2H) assays were performed to screen the potential receptor of MCP03 following the standard protocol [31] that was schematically illustrated in Supplementary Figure S1. Briefly, a cDNA library from *C. elegans* was constructed using the plasmid vector pGADT7 and transformed into a yeast strain Y187. Full-length MCP03 was fused to the GAL4 DNA binding domain in the vector pGBKT7 to yield the recombinant plasmid pMB832 (Supplementary Figure S2), and was transformed into the yeast host strain Y2H Gold to yield the recombinant MB832. Two-hybrid interactions were screened by mating MB832 with A.D. fusion *C. elegans* cDNA library. Blue colonies on SD/-Trp-Leu medium supplemented with X-*α* Gal and AbA were further analyzed on SD/-Trp-Leu-His-Ade/X-*α* Gal/AbA (QDO/X/A) medium. The resultant clones that appeared on QDO/X/A medium were subjected to colony PCR using specific primers to identify the interacting partners. The resultant *csn-5* was cloned into the vector pGADT7, and the interaction with MCP03 was tested in a Y2H X-gal assay [31].

2.6. Expression and Purification of Recombinant Proteins from C. elegans

Total RNA was extracted from the wild-type strain N2 of *C. elegans* using the Trizol method [32]. Subsequently, cDNA synthesis was performed using the TransScript One-Step gDNA Removal and

 doi:10.20944/preprints202308.1827.v1

cDNA Synthesis SuperMix (TransGen Biotech). Briefly, the gene *csn-5* was amplified using the F-pGEX-6P-1-*csn*-5 and R-pGEX-6P-1-*csn*-5 primers (Supplementary Table S1) and then cloned into the expression vector pGEX-6P-1 using Gibson one-step assembly method [33] to generate the recombinant pMB833 (Supplementary Figure S3), which was transformed into *E. coli* BL21(DE3) to yield recombinant *E. coli* MB833. For induced CSN-5 expression, MB833 cells were cultured in LB broth until reaching an OD_{600} of 0.6 at 37 °C, then 0.2 mmol L^{-1} IPTG was added and the cultures were further incubated for 4 h at 30 °C. The recombinant protein was purified using affinity chromatography with glutathione Sepharose 4B. The eluted protein was subsequently dialyzed and stored at –80 °C.

2.7. Scanning Electron Microscope (SEM)

The worm surface morphology of *C. elegans* N2 and MCP03-treated N2 was observed under an SEM (JSM-6390/LV, JEOL, Japan) following the previously described sample preparation and fixation procedures [34].

2.8. Pull-Down Assay

E. coli MB831 and MB833 expressing His-tag fused MCP03 and glutathione S-transferase (GST) tagged CSN-5, respectively, and *E. coli* MB830 harboring plasmid pGEX-6P-1 (as the negative control) were IPTG-induced following above protocols. Cells were harvested by centrifugation at 12000 rpm for 10 min at 4 °C, then were resuspended with PBS (pH 7.4), and were homogenized using a high-pressure homogenizer (NS1001L 2K, Niro Soavi, Germany) at 1000 *psi*. Following centrifugation of the disrupted suspensions, the supernatants from MB831/MB833 and MB831/MB830 (negative control) were grouped to incubate with glutathione-coupled Sepharose beads in a rotative incubator for 3 h at 4 °C, and were centrifuged, followed by washing the beads with pre-cooled (4 °C) PBS (pH 7.4) for at least 5 times to elute unbound proteins. The bead-bound proteins were detected using 12.5% SDS-polyacrylamide gel electrophoresis (PAGE) and Western blot analysis with an anti-His tag antibody, following the standard protocols [26].

2.9. Western Blot Analysis

To analyze the expression of MCP03 in *E. coli* MB831, and the binding interaction between MCP03 and CSN-5, after the separation of total proteins via 10% and 12.5% SDS-PAGE, respectively, the gels were electro-transferred to a nitrocellulose membrane, were then incubated overnight with a 1:11000 dilution of anti-His tag antibody, followed by incubation with an HRP-conjugated secondary antibody at a 1:1500 dilution. The membrane was visualized using an enhanced chemiluminescence substrate as described by the manufacturer (Biorad Hercules, CA, USA).

2.10. Construction of csn-5 RNAi Strain

An RNAi strain (namely *E. coli* MB834) was constructed and was used for silencing *csn-5* expression in *C. elegans* N2 following a previously described protocol [35]. The *csn-5* fragment was PCR-amplified from the cDNA of *C. elegans* N2 using the primers F-RNAi.*csn*-5 and R-RNAi.*csn-5* (Supplementary Table S1), the amplified fragment was then digested with *Hin*d III, and was cloned into an RNAi plasmid vector pL4440 to yield recombinant pMB834 (Supplementary Figure S4A), which was transformed into *E. coli* HT115 to generate *E. coli* MB834. The expression of dsRNA in MB834 was induced with 1 mmol L^{-1} IPTG at the final concentration (Supplementary Figure S4B).

2.11. Co-Localization

The rhodamine (Rho) labeled MCP03 was fed to GFP-labeled transgenic *C. elegans* LG333 (*skn-1b*::*gfp*) strain for 48 h. The labeling of MCP03 with Rho was performed according to a previous protocol [6]. The fluorescent morphology of individual worm was observed under a Confocal Laser Scanning Microscope (CLSM) (N-STORM, Nikon, Japan) using GFP and RFP modes. The co-

 doi:10.20944/preprints202308.1827.v1

localization was confirmed by the merged GFP and RFP fluorescence. *C. elegans* LG333 (*skn-1b*::*gfp*) strain fed with *E. coli* OP50 cells was used as the control.

2.12. Real-Time Quantitative PCR (RT-qPCR)

Synchronized *C. elegans* N2 L4 stage worms were fed with the purified MCP03 or BSA (negative control). The worms were collected at the 24 h after feeding, and were used for extracting total RNAs according to a previously reported protocol [32]. RT-qPCR was performed to determine the expression levels of selected *C. elegans* genes using the comparative cycle threshold method ($2^{-\triangle\triangle C.T.}$ method) [36]. The primers used for RT-qPCR analysis of the selected genes were listed in Supplementary Table S1. The gene *GAPDH* was used as an internal reference gene, while RNAs from BSA-fed *C. elegans* N2 were used as the negative control.

2.13. Data Analysis

Statistical analysis was performed using GraphPad Prism 8.3 (GraphPad Software, LLC, Boston, MA, USA), and data were derived from at least three biological replicates unless otherwise indicated. $p < 0.05$ was defined as statistical significance.

3. Results

3.1. Molecular Characterization, Expression and Purification, and Nematicidal Activity of MCP03

The gene *mcp03* (gene locus *"VT47_10710"*) from the genome of *P. syringae* MB03 was characterized using the online tool BLASTn in the GenBank nucleotide sequence database at the National Centre for Biotechnology Information (NCBI) server (https://blast.ncbi.nlm.nih.gov/Blast.cgi). The MCP03 protein was predicted to encode a 598 amino acid (AA) protein with a theoretical molecular weight (Mw) of approximately 66 kDa. Conserved domain architecture analysis revealed that MCP03 contains two domains: a HAMP domain, spanning AAs 93 to 149, and an MCP signal domain, spanning AAs 154 to 424 (Figure 1B). The gene *mcp03* was amplified from the *P. syringae* MB03 genome, and its sequence was confirmed to be identical to that of the open reading frame (ORF). Figure 1A(b) showed that an additional band with a molecular mass apparently equal to that of the predicted MCP03 was present in the *E. coli* MB831 profile (indicated by arrow) but was not found in the BL21(DE3) profile (the negative control), indicating the successful expression of MCP03 in *E. coli* MB831 cells. Subsequently, a liquid-based bioassay was performed to evaluate the virulence potential of *E. coli* MB831 intact cells toward *C. elegans*. As shown in Figure 1A(c), MB831 exhibited pronounced nematicidal activity against *C. elegans* compared with that of the negative control *E. coli* BL21(DE3) cells (*P. syringae* MB03 intact cells were used as a positive control). Therefore, the MCP03 protein expressed in MB831 was purified, and the product was subjected to SDS-PAGE [Figure 1C(a)] and Western blot analysis [Figure 1C(b)], which confirmed MCP03 was purified as alone protein component at high purity. Thus, we further evaluated the nematicidal activity of the purified MCP03 against *C. elegans*. Figure 1D shows the purified MCP03 exhibited significant nematicidal activity against *C. elegans* in a dose-dependent pattern, with a calculated LC_{50} value of 124.47 (99.22–147.47) μg mL^{-1}, indicating the high toxicity of this protein against *C. elegans*.

3.2. MCP03 Affects Different Phenotypes of C. elegans

The effects of purified MCP03 on the spawning number and growth of *C. elegans* N2 were investigated to further evaluate the virulence of this protein, using BSA as the negative control. Figure 2A shows that MCP03 exhibited a significant detrimental effect on the brood size of worms following the increased dose from 0 to 120 μg mL^{-1}, and the spawning rate declined to 0 under 120 μg mL^{-1} MCP03, indicating that feeding of MCP03 caused pathogenic impairment on the reproductive system of *C. elegans* N2. Moreover, Figure 2B shows that low MCP03 concentration (lower than 20 μg mL^{-1}) had only slight repressive effect on the size of the synchronized L1-stage *C. elegans* worms; however, higher MCP03 concentrations caused the greater decrease of worm size, and at 120 μg mL^{-1} of MCP03,

Preprints (www.preprints.org) | NOT PEER-REVIEWED | Posted: 29 August 2023 doi:10.20944/preprints202308.1827.v1

the area of the worm was only 20 % compared with that of the control BSA, thereby indicating a dose-dependent detrimental effect of MCP03 on the growth of *C. elegans*.

Interestingly, MCP03 also exerted disruptive impairment on the surface cuticles of *C. elegans* N2, as severe depressed dents and wrinkles of the cuticles were clearly visualized under SEM on the surface phenotype of worms fed with MCP03 in 72 h, which strongly contrast to the smooth surface of worms fed with BSA (Figure 2C).

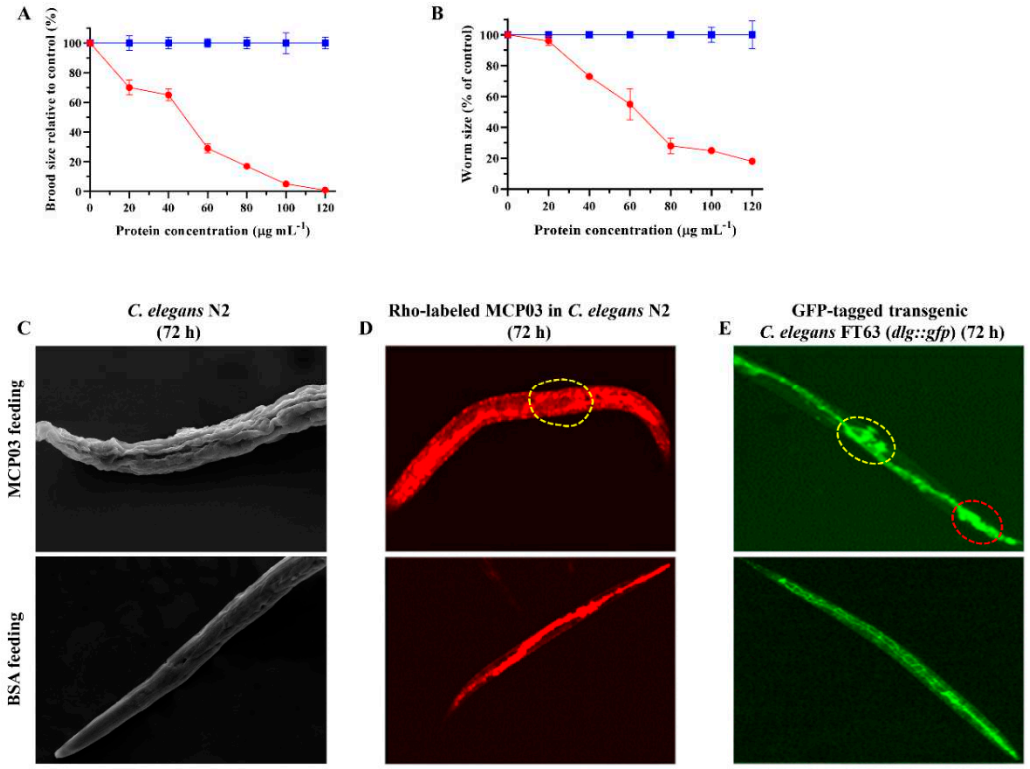

Figure 2. Detrimental effects of MCP03 on *C. elegans* N2. (**A**) Brood size assay of *C. elegans* under different concentrations of MCP03. (**B**) Worm size assay of *C. elegans* treated with different doses of MCP03. (**C**) SEM micrography of surface morphology of *C. elegans* after feeding with MCP03 or BSA. (**D**) Fluorescence micrography of Rho-labelled *C. elegans* N2 fed with MCP03. Rho-labelled BSA was used as the negative control. The yellow dotted-circle region indicates the destructive intestinal tract. (**E**) Fluorescence micrography of GFP-tagged *C. elegans* FT63 (*dlg::gfp*) fed with MCP03. The yellow dotted-circle region indicates the impaired ovary, and the red dotted-circle region indicates the destructive intestinal tissues.

To investigate whether MCP03 acted on the intestinal tract of worms, we examined the intestinal morphology of two *C. elegans* worms that were fed with Rho-labeled MCP03 in 72 h: the wild-type N2 and GFP-tagged FT63 (*dlg*::*gfp*). Figure 2D shows that the intestinal tract of N2 that was treated with MCP03 appeared to be pathologically changed under the upper CLSM micrography, as disseminative red fluorescence distributed throughout the entire worm body, and some destructive structures were distinctly visible in the intestinal tract (indicated by dotted-circle region), while the control N2 fed with Rho-labeled BSA displayed red fluorescence confined to only the intestinal tract. Moreover, the destructive effect on the integrity of epithelial junctions of worms by feeding MCP03 was also confirmed by MCP03-treated FT63(*dlg*::*gfp*) worms, as significant disruption of epithelial junctions was clearly visible under the upper CLSM micrography (Figure 2E) (indicated by red dotted-circle region), whereas the control worm fed with BSA exhibited an integrated intact bamboo-shaped intestinal tract. It is noteworthy that the disseminative GFP fluorescence was found in the ovary region of the MCP03-treated FT63 (*dlg*::*gfp*) worm (indicated by yellow dotted-circle region), an apparent impairment on this organ by feeding MCP03, which is conducive to explaining the detrimental effect of MCP03 on the reproductive functionality of *C. elegans*.

Preprints (www.preprints.org) | NOT PEER-REVIEWED | Posted: 29 August 2023 doi:10.20944/preprints202308.1827.v1

3.3. Identification of CSN-5 As A Putative Receptor of MCP03

To identify the receptor protein that interacts with MCP03 to potentially actuate the pathogenicity of *C. elegans* N2, we performed an N2 genome-wide yeast two-hybrid (Y2H) screening with MCP03 as the bait. Figure 3A shows a typical trilobite pattern of mating yeast cells, indicating the successful mating of MB832 and the Y187 Y2H library cells carrying various fractions of *C. elegans* cDNA; Figure 3B shows blue colonies on QDO/X/A plates, indicating that the presence of potential prey proteins interacting MCP03 in these colonies. Therefore, these four colonies were subjected to PCR amplification of their harbored prey cDNAs, which showed that all four prey cDNA fragments were in similar size in the electrophoresis profiles (approximately 1100 bps) (Figure 3C). These fragments were sequenced, and were found to be an identical ORF consisting of 1107-bp nucleotide sequences, which can be further identified as the *csn-5* gene of *C. elegans* by searching the WormBase database (https://wormbase.org//). The predicted protein CSN-5 is composed of 369 AA with a theoretical Mw of ~67 kDa, and is a key subunit of a subunit of a COP9 signalosome, a conserved protein complex that plays critical roles in regulating gene expression, cell proliferation, and cell cycle of eukaryotes [37]. Conserved domain architecture analysis revealed that CSN-5 has an MPN superfamily domain (AA45–AA292), which contains three motifs, Mov34/MPN/JAMM, and a Zinc binding site with metalloproteinase activity (Figure S5A). The three-dimensional structure modeling of CSN-5 shows it contains multiple α-helices and β-sheets that constitute a barrel fold. These structural characteristics suggest the potential of CSN-5 in functionally involved in the interaction with other proteins.

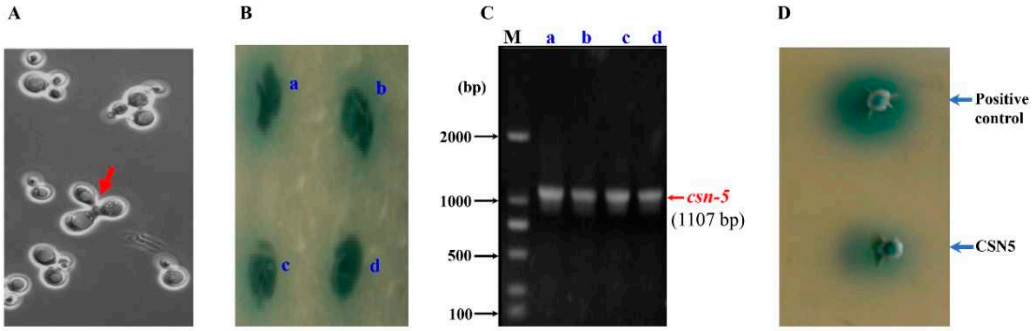

Figure 3. Yeast Two-hybrid assay for the identification of MCP03 interacting receptor. (**A**) Micrography of the mating yeast cells. The red arrow indicates a typically successful trilobite mating pattern. In (**B**), (a)–(d) indicate positive colonies in the preliminary screening on QDO/X/A medium plate. (**C**) Electrophoresis of PCR-amplified plasmid cDNAs from positive colonies. Lane M, DNA Mw marker. Lane (a)–(d), PCR-amplified products from the colony a–d on (B). (**D**) Yeast response validation on CSN-5 by co-transformation of bait plasmid pMB832 and prey plasmid pGADT7-*csn-5* into Y187.

3.4. In Vivo and In Vitro Binding Interaction of MCP03 with CSN-5

An *in vivo* yeast response validation on CSN-5 by co-transformation of bait plasmid pMB832 and prey plasmid pGADT7-*csn-5* into Y187 showed positive colony by CSN-5 (Figure 3D), thereby in principle verifying the binding between CSN-5 and MCP03. *In vitro* Pull-down affinity chromatography assay and Western blot analysis were also performed to confirm the binding activity of the purified GST-tagged CSN-5 protein (GST-CSN-5) and MCP03. Figure 4A shows GST-CSN-5 was successfully expressed in *E. coli* MB833, with the predicted Mw of ~ 67 kDa (Figure 4A, lane 2 indicated by blue arrow), while His-tagged MCP03 was expressed in MB831 at the Mw of ~ 66 kDa (Figure 4A, lane 3 indicated by red arrow). After co-incubation of the purified GST-CSN-5 and MCP03, they formed a binding complex that was identified in the SDS-PAGE profile (Figure 4A, lane 5), whereas no detected binding complex occurred in the co-incubation of alone GST and MCP03 (Figure 4A, lane 4). Western blot analysis using a specific anti-His antibody further visualized an ~ 67 kDa positive band in the GST-CSN-5/MCP03 complex, a little higher than that of the control

Preprints (www.preprints.org) | NOT PEER-REVIEWED | Posted: 29 August 2023 doi:10.20944/preprints202308.1827.v1

MCP03 at ~ 66 kDa, which appeared to be caused by the complex formed with GST-CSN-5 at relatively higher Mw. Collectively, these results confirm the binding activity between MCP03 and CSN-5.

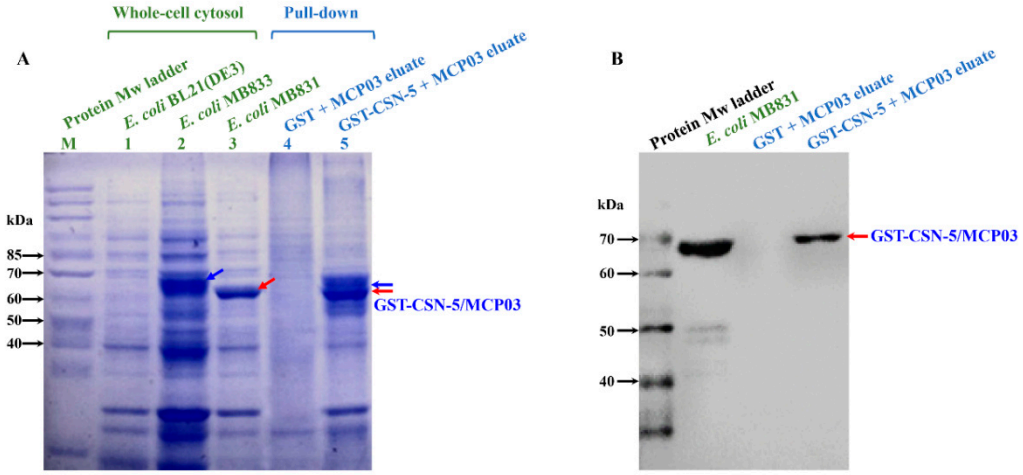

Figure 4. Binding interaction between MCP03 and CSN-5. (**A**) SDS-PAGE analysis of recombinant *E. coli* cells expressing CSN-5 and *in vitro* Pull-Down assay of MCP03 and CSN-5 interaction. (**B**) Western blot analysis of the Pull-Down fractions.

We further investigated *in vivo* co-localization of CSN-5 and MCP03 in *C. elegans* to verify CSN-5 bound to MCP03 as a receptor protein. Several previous studies have revealed that the proteins CSN-5 and SKN-1 were localized in the cell nucleus of *C. elegans* [38,39]. Due to the current unavailability of a CSN-5::GFP strain, we employed a *C. elegans* SKN-1::GFP strain (namely, LG333 (*skn-1b*::*gfp*)) as a substitute. After 72 h of feeding LG333 worms with Rho-labeled MCP03, the CLSM observations showed clear *in-situ* overlapped green and red fluorescence that can be merged as notable yellow coloration (Figure 5), indicating that co-localization between the Rho-labeled MCP03 and GFP-labeled SKN-1 (which refers to Rho-labeled MCP03 and CSN-5) within the *C. elegans*.

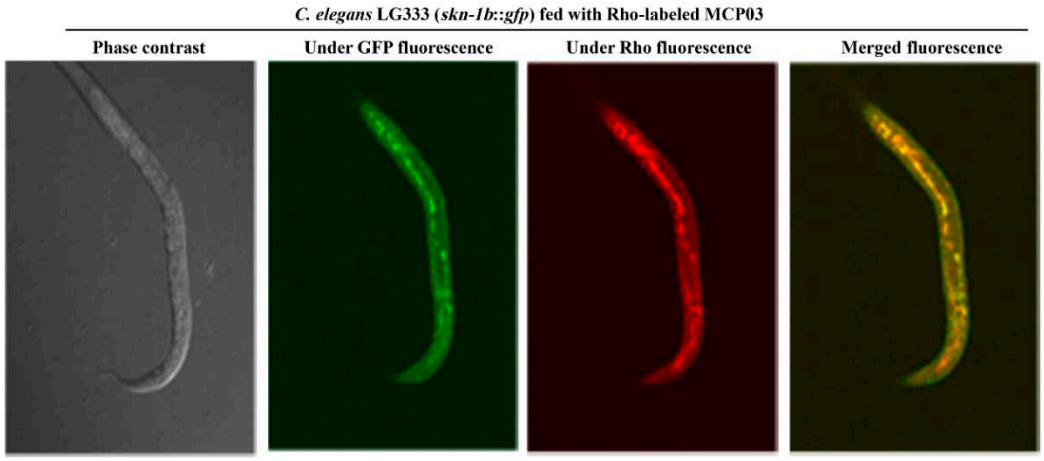

Figure 5. Co-localization analysis MCP03 and CSN-5 protein in *C. elegans* LG333 (*skn-1b*::*gfp*) strain. The captured GFP and RFP images were merged using Image J software. Yellow color refers to the binding interaction between MCP03 and CSN-5.

3.5. Effects of Silencing csn-5 by RNAi on Brood Size, Growth Size, and Cuticle Integrity

RNAi experiments were performed to silence *csn-5* of *C. elegans* N2 (the RNAi-treated *C. elegans* N2 was named "N2-CSN-5-RNAi"), then compared the N2-CSN-5-RNAi with N2 in terms of growth,

Preprints (www.preprints.org) | NOT PEER-REVIEWED | Posted: 29 August 2023 doi:10.20944/preprints202308.1827.v1

brood size, and cuticle morphology. The *csn-5* gene of N2 was cloned to pL4440 to construct pMB834, and a 1273-bp dsRNA specific for *csn-5* RNAi was synthesized upon IPTG induction in *E. coli* MB834 cells harboring pMB834 (Figure S4B). The *C. elegans* N2-CSN-5-RNAi worms were yielded by feeding this dsRNA to N2. Figure 6 shows only a limited effect of *csn-5* RNAi on the growth of N2 under microscopic observations (Figure 6A) and measured average individual size (Figure 6B) of two worms, indicating that CSN-5 did not significantly involve in regulating the growth of *C. elegans*. However, the RNAi on *csn-5* caused a significant inhibitory effect on the brood size of N2-CSN-5-RNAi compared to N2, as the N2-CSN-5-RNAi worms laid approximately 65% decrease of eggs compared with that of the wild-type N2 ($p < 0.05$) (Figure 6C), indicating that CSN-5 served as the action receptor of MCP03 in suppressing the reproduction system of *C. elegans*. Moreover, the *csn-5* RNAi caused morphological changes in the surface cuticles of worms, as the crumples and depressed dents of the cuticles were clearly visible in the N2-CSN-5 RNAi worms (Figure 6D, indicated by red arrow), in consistent with the similar pathological pattern of MCP03 treatment (Figure 6D), further identifying that CSN-5 is functional action acceptor of MCP03.

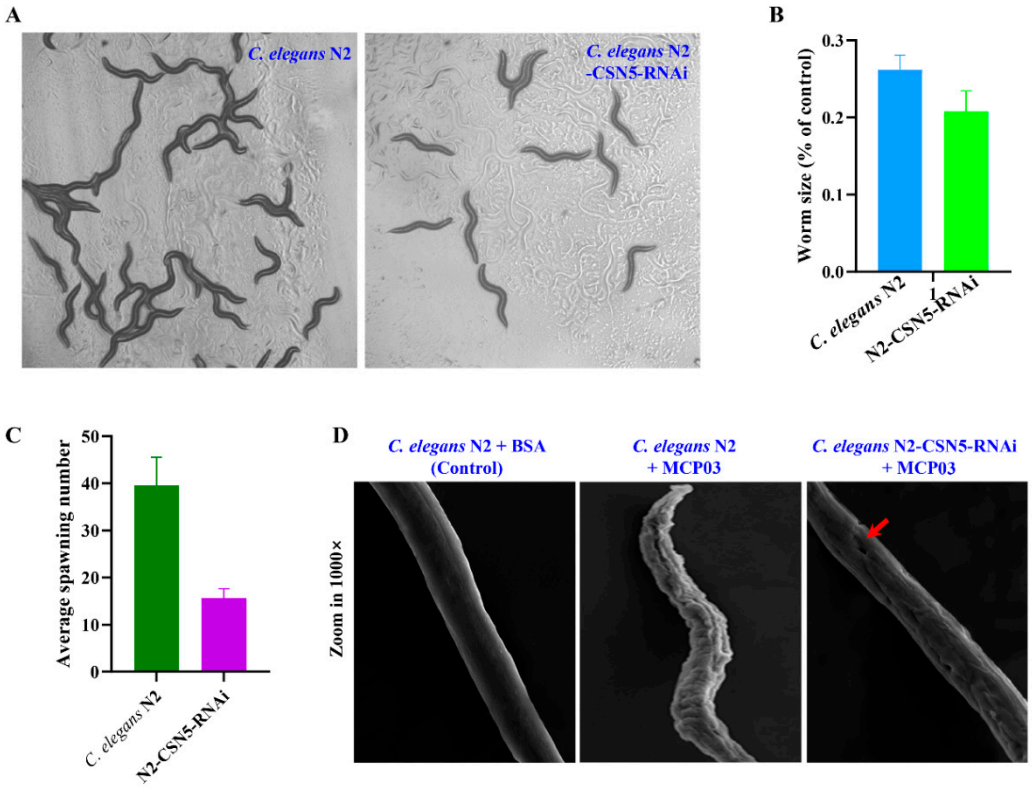

Figure 6. Effects of *csn-5* RNAi on the worm size, brood size, and surface cuticle of *C. elegans* N2. (**A**) Worm size assay of the wild-type and *csn-5* RNAi treated *C. elegans* N2 worms. (**B**) Worm size quantification of the wild-type and *csn-5* RNAi-treated *C. elegans*. (**C**) Quantification of the average spawning number of the wild-type and *csn-5* RNAi-treated *C. elegans*. (**D**) SEM micrography of the *csn-5* RNAi-treated *C. elegans* worms fed with MCP03. The wild-type N2 worms fed with BSA and MCP03 were used as the negative and positive control, respectively. The red arrow indicates the depressed dent of the worm surface.

3.6. RT-qPCR Analysis of Selected Genes of N2

RT-qPCR analysis of several selected genes relative to growth, brood size, and cuticle formation in *C. elegans* was performed to investigate gene expression levels following MCP03 treatments. These genes include *col-117*, which encodes a collagen belonging to the Col-3 family, and serves as a main component of stratum corneum on the *C. elegans* surface [40]; *kgb-1*, a gene involved in regulating the reproductive function of *C. elegans* [41]; *unc-98*, a gene involved in the assembly and maintenance of

Preprints (www.preprints.org) | NOT PEER-REVIEWED | Posted: 29 August 2023 doi:10.20944/preprints202308.1827.v1

myofibrils [42,43]; and *mpk-1*, a gene involved in regulating the resveratrol-mediated longevity of *C. elegans* through MPK-1 signaling pathways [44]. Figure 7 shows after feeding MCP03 for 24 h, the expression levels of *col-117*, *kgb-1* and *unc-98* in *C. elegans* N2 were significantly downregulated, while *mpk-1* was significantly upregulated, and *csn-5* remained unchanged. Apparently, the downregulation of *col-117* expression is consistent with the observed depressed morphology of stratum corneum on the worm surface after feeding MCP03 (Figure 6D); the down-expression of *kgb-1* affected the fertility of worms, as identified previously, as both KGB-1 and CSN-5 interacted with GLH-1 and regulated the reproductive function of nematodes [43]; and the down-expression of *unc-98* affected the formation of *C. elegans* muscle tissue [45]. Collectively, these results suggest that MCP03 bound to CSN-5 actuated multiple signal pathways to regulate significant genes relative to the growth, reproduction, and worm morphology.

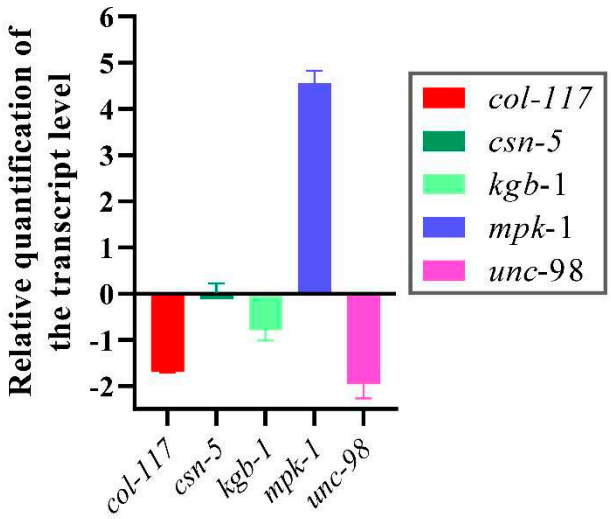

Figure 7. RT-qPCR of expression activities of several selected genes relative to fertility, growth, and cuticle formation of *C. elegans*.

4. Discussion

This study aimed to investigate the action mechanism underlying the nematicidal activity of MCP03, a methyl-accepting chemotaxis protein, in the *P. syringae* MB03-*C. elegans* infection model. We evaluated not only the direct nematicidal activity of MCP03 against *C. elegans*, but also the detrimental effects on the growth, brood size, and external and internal morphology of *C. elegans*. We identified CSN-5 as an MCP03-binding protein in *C. elegans*. Although the role of MCPs as key players in chemotaxis and pathogenicity has been well-characterized in different bacteria [14], this study for the first time provides new insights into the nematicidal activity and action mechanism of a bacterial MCP against nematodes.

In *P. syringae* MB03 genome, total of 46 MCP-encoding genes (chemoreceptor genes) were annotated. Interestingly, the genome-wide prediction of nematicidal genes of *P. syringae* MB03 showed the nematicidal potential of MCP03 among these MCPs [23]. In consistent with this prediction, the bioassays of heterologously expressed MCP03 exhibited a significantly lethal activity again *C. elegans*, with an LC_{50} of 124.47 (99.22~147.47) μg mL^{-1}, and multiple detrimental effects on the growth, reproduction, and morphology of *C. elegans*. Although the activity is relatively lower than that of Cry5Da1, a well-known eminent bacterial nematicidal toxin of *B. thuringiensis* with an LC_{50} of 36.69 μg mL^{-1} against *C. elegans* [46], given the multifaceted nematode-toxic activities, MCP03 still holds promise as a potential nematode-pest control agent for pursuing in agricultural, horticultural or forestry applications.

A subunit of COP9 signalosome, CSN-5, is primarily localized in the cytoplasm and nucleus as its interacting partner. *C. elegans* contains seven CSN subunits; CSN 1, 2, 3, 4, and 7 possess PCI

 doi:10.20944/preprints202308.1827.v1

domains that promote protein-protein interactions and have nucleic acid binding properties [47]. In contrast, CSN-5 and CSN-6 possess an MPN domain with a JAMM (Jab/MPN/Mov34) sequence and exhibit metalloproteinase activity [48]. CSN-5 is also involved in ubiquitin-dependent protein degradation, regulation of the cell cycle, and also regulate multiple signal transduction processes [49]. In the current study, CSN-5 was identified as the binding receptor of MCP03 through multiple *in vitro* and *in vivo* experiments. The data shown in Figure 2 indicate that MCP03 targeted the intestinal tissues of N2, and caused severe destructive impairment on the integrity of epithelial junctions and other organs (such as the ovary). We currently presume that these pathological changes could be the main lethal determinants of MCP03 treatment, as these changes definitely associated with other stepwise pathological processes, such as the decrease of food intake, the collapse of substance and energy metabolisms, the occurrence of septicemia, among others, which ultimately led to the death of *C. elegans*. However, whether these pathological processes were related to the binding of MCP03 and CSN-5 remained unknown. Further studies are required to elucidate the role and action mechanism of the MCP03-CSN-5 binding complex in the pathogenesis of MCP03 targeting the intestinal tract of worms.

Several investigations have demonstrated that CSN-5 interacted with UNC-98 and UNC-96 involved in the assembly and maintenance of myofibers [42]. The outer surface of MCP03-treated N2 was severely shrunk (Figure 2C), the expression of *col-117* and *unc-98* was significantly downregulated (Figure 7), and the CSN-5 RNAi-silenced worms retrieved surface cuticle integrity to an extent (Figure 6D). These results suggest that MCP03 interacts with CSN-5, resulting in the downregulation of the expression of collagen and certain muscle-related proteins, and causing the severely depressed wrinkles of the worms' surface. Additionally, MCP03 also suppressed the brood size to a lesser extent (Figure 2A), and RNAi with *csn-5* significantly reduced the spawning rate of N2 (Figure 6C), confirming the critical role of CSN-5 in regulating the fertility activity of *C. elegans*, which could be attributed to the downregulation of the *kgb-1* expression, as CSN-5 and KGB-1 are capable of regulating the expression of GLH-1 which is crucial for the fertility of *C. elegans* [41]. It is noteworthy that the expression of *csn-5* in N2 remained unchanged following MCP03 treatment. We speculate that MCP03 was bound to CSN-5, and enabled inhibiting its activity to some extent without significantly reducing the protein's expression. However, it is possible that MCP03 has other but undetected receptors in *C. elegans*, owing to the coverage limitations of the cDNA library and insufficient screening processes in the current study.

Based on the results obtained in this study, we propose the following outline for the pathogenicity of MCP03 against *C. elegans*. Following the entry of MCP03 into the intestinal tract of *C. elegans* by feeding, MCP03 entered the intestinal epithelial cells, thereby triggering the physiological and pathological changes of the epithelial cells, leading to a series of lesions such as intestinal perforation, disruption of osmotic balance, and destruction of partial intestinal tissues, ultimately causing the death of *C. elegans* worms. Meanwhile, MCP03 bound to its receptor protein CSN-5 to form an MCP03-CSN-5 complex in some target cells, thereby activating multiple signaling pathways, including downregulating the genes *col-117*, *kgb-1* and *unc-98*, and upregulating other genes including *mpk-1*, among others. The activity changes ultimately lead to adverse effects on the fertility capability, growth, and cuticle integrity of *C. elegans*. Of these continuous signaling pathways, some behind signaling molecules, such as DAF-16, MPK-1, and GLH-1, etc., which activating various subsequent pathological lesions following the MCP03-CSN-5 binding are conducive for pathogenesis. In fact, DAF-16 has been proved to be positively regulated when worms were infected and the epidermis were damaged [50]; MPK-1 was able to promote resveratrol-mediated nematode lifespan in a non-dependent manner through the SIR-2.1/DAF-16 (closely related to regulating nematode lifespan and immunity) pathway by regulating the accumulation of SKN-1 in the nucleus [44]. It is therefore of particular interest to further investigate the signaling pathways underlying the interactions of these proteins that function as signaling molecules to actuate the pathogenesis of *C. elegans* worms; such an investigation is now one of our primary goals.

Preprints (www.preprints.org) | NOT PEER-REVIEWED | Posted: 29 August 2023 doi:10.20944/preprints202308.1827.v1

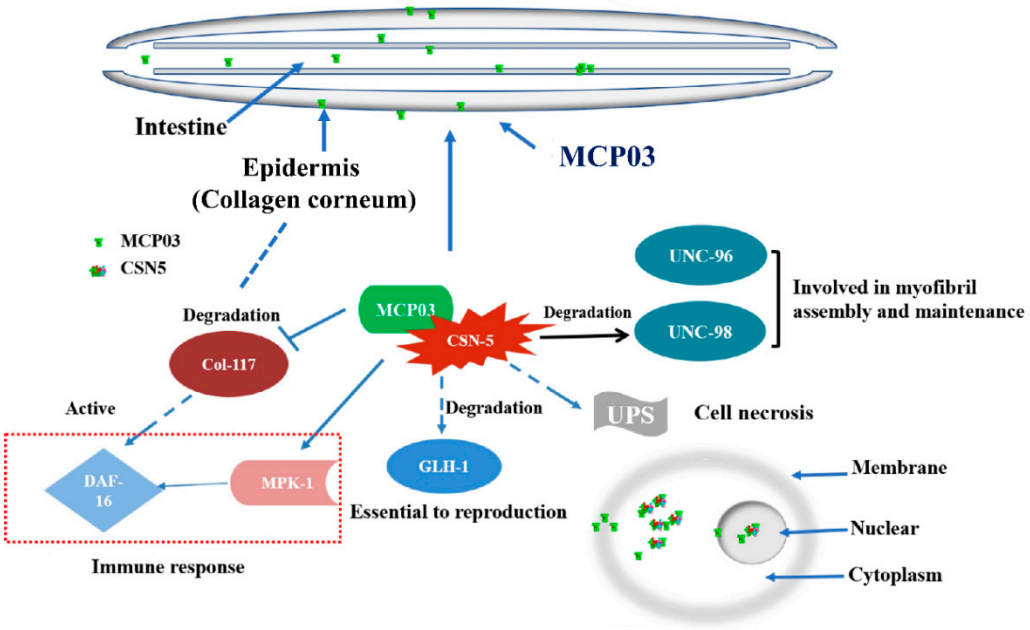

Figure 8. The proposed action mechanism underlying MCP03 pathogenicity against *C. elegans*.

5. Conclusions

The current study demonstrates the significant nematicidal activity of MCP03 against *C. elegans*, and the detrimental effects on the intestinal tissues, fertility capability, growth, and surface cuticle morphology. Through Y2H assays, a subunit of the CSN signaling complex, CSN-5, was identified as an action receptor of MCP03. The binding interaction between MCP03 and CSN-5 was confirmed through *in vitro* pull-down and *in vivo* co-localization assays on different tagged worms. Following the RNAi on *csn-5* of *C. elegans*, several genes relative to fertility, growth, and cuticle formation were found to be downregulated in MCP03-treated worms. Due to its relatively high nematicidal virulence and multiple detrimental activities, MCP03 holds the potential to be pursued for development of a bionematicide.

Supplementary Materials: The following supporting information can be downloaded at the website of this paper posted on Preprints.org, Figure S1: Schematic illustration of yeast two-hybrid system used for identification of MCP03-binding receptor protein; Figure S2: The construction and verification of recombinant plasmid pMB832 expressing the *mcp03* gene; Figure S3: The construction and verification of recombinant plasmid pMB833 expressing the *csn-5* gene; Figure S4: The construction of pMB834 and verification of the expression of dsRNA in yeast MB834; Figure S5: Structural illustration of conserved domains and the predicted three-dimensional configuration of the CSN-5 protein; Table S1: Bacterial, yeast and nematode strains, plasmids and oligonucleotide primers used in this study.

Author Contributions: Conceptualization, L.L., L.X. and J.L.; methodology, J.L., H.D., A.B. and Z.W.; validation, J.L. and H.D.; formal analysis, H.D., Y.A. and A.B.; investigation, J.L., H.D., A.B., Z.W. and X.Y.; data curation, J.L., H.D., A.B., Y.A. and L.L.; writing—original draft preparation, J.L., H.D. and A.B.; writing—review and editing: L.L. and X.Y.; supervision, L.L. and L.X.; funding acquisition, J.L and L.L. All authors have read and agreed to the published version of the manuscript.

Funding: This work was funded by a grant from Meizhou City's 2021 Guangdong Provincial Rural Revitalization Strategy Special Fund (Grant no. 2021A0305002), a grant from Guangdong Provincial Science and Technology Innovation Strategy Special Fund (Grant no. KTP20210213), and a grant from Guangdong Pomelo Engineering Technology Development Center, Guangdong Provincial Key Scientific Research Platform Construction Project of Regular University (Grant no. 2019GCZX007).

Institutional Review Board Statement: Not applicable.

Data Availability Statement: Data available in a publicly accessible repository.

Conflicts of Interest: The authors declare that they have no conflicts of interest.

References

1. Abad, P.; Gouzy, J.; Aury, J. M.; Castagnone-Sereno, P.; Danchin, E. G.; Deleury, E.; Perfus-Barbeoch, L.; Anthouard, V.; Artiguenave, F.; Blok, V. C.; Caillaud, M. C.; Coutinho, P. M.; Dasilva, C.; De Luca, F.; Deau, F.; Esquibet, M.; Flutre, T.; Goldstone, J. V.; Hamamouch, N.; Hewezi, T.; Jaillon, O.; Jubin, C.; Leonetti, P.; Magliano, M.; Maier, T. R.; Markov, G. V.; McVeigh, P.; Pesole, G.; Poulain, J.; Robinson-Rechavi, M.; Sallet, E.; Ségurens, B.; Steinbach, D.; Tytgat, T.; Ugarte, E.; van Ghelder, C.; Veronico, P.; Baum, T. J.; Blaxter, M.; Bleve-Zacheo, T.; Davis, E. L.; Ewbank, J. J.; Favery, B.; Grenier, E.; Henrissat, B.; Jones, J. T.; Laudet, V.; Maule, A. G.; Quesneville, H.; Rosso, M. N.; Schiex, T.; Smant, G.; Weissenbach, J.; Wincker, P., Genome sequence of the metazoan plant-parasitic nematode *Meloidogyne incognita*. *Nat Biotechnol* **2008,** *26*, 909–915.
2. Topalović, O.; Geisen, S., Nematodes as suppressors and facilitators of plant performance. *New Phytol* **2023,** *238*, 2305–2312.
3. Castillo, P.; Navas-Cortés, J. A.; Landa, B. B.; Jiménez-Díaz, R. M.; Vovlas, N., Plant-parasitic nematodes attacking chickpea and their in planta interactions with rhizobia and phytopathogenic fungi. *Plant Dis* **2008,** *92*, 840–853.
4. Sabbahi, R.; Hock, V.; Azzaoui, K.; Saoiabi, S.; Hammouti, B., A global perspective of entomopathogens as microbial biocontrol agents of insect pests. *J Agric Food Res* **2022,** *10*, 100376.
5. Luo, H.; Xiong, J.; Zhou, Q.; Xia, L.; Yu, Z., The effects of *Bacillus thuringiensis* Cry6A on the survival, growth, reproduction, locomotion, and behavioral response of *Caenorhabditis elegans*. *Appl Microbiol Biotechnol* **2013,** *97*, 10135–10142.
6. Peng, D.; Lin, J.; Huang, Q.; Zheng, W.; Liu, G.; Zheng, J.; Zhu, L.; Sun, M., A novel metalloproteinase virulence factor is involved in *Bacillus thuringiensis* pathogenesis in nematodes and insects. *Environ Microbiol* **2016,** *18*, 846–862.
7. Dubern, J. F.; Cigana, C.; De Simone, M.; Lazenby, J.; Juhas, M.; Schwager, S.; Bianconi, I.; Döring, G.; Eberl, L.; Williams, P., Integrated whole-genome screening for *Pseudomonas aeruginosa* virulence genes using multiple disease models reveals that pathogenicity is host specific. *Environ Microbiol* **2015,** *17*, 4379–4393.
8. Sun, X.; Zhang, R.; Ding, M.; Liu, Y.; Li, L., Biocontrol of the root-knot nematode *Meloidogyne incognita* by a nematicidal bacterium *Pseudomonas simiae* MB751 with cyclic dipeptide. *Pest Manag Sci* **2021,** *77*, 4365–4374.
9. Phani, V.; Shivakumara, T. N.; Davies, K. G.; Rao, U., *Meloidogyne incognita* fatty acid- and retinol-binding protein (Mi-FAR-1) affects nematode infection of plant roots and the attachment of *Pasteuria penetrans* endospores. *Front Microbiol* **2017,** *8*, 2122.
10. Tedesco, P.; Di Schiavi, E.; Esposito, F. P.; de Pascale, D., Evaluation of *Burkholderia cepacia* complex bacteria pathogenicity using *Caenorhabditis elegans*. *Bio Protoc* **2016,** *6*, e1964.
11. Huang, X.; Tian, B.; Niu, Q.; Yang, J.; Zhang, L.; Zhang, K., An extracellular protease from *Brevibacillus laterosporus* G4 without parasporal crystals can serve as a pathogenic factor in infection of nematodes. *Res Microbiol* **2005,** *156*, 719–727.
12. Crickmore, N., Using worms to better understand how *Bacillus thuringiensis* kills insects. *Trends Microbiol* **2005,** *13*, 347–350.
13. Wadhams, G. H.; Armitage, J. P., Making sense of it all: Bacterial chemotaxis. *Nat Rev Mol Cell Biol* **2004,** *5*, 1024–1037.
14. Salah Ud-Din, A. I. M.; Roujeinikova, A., Methyl-accepting chemotaxis proteins: A core sensing element in prokaryotes and archaea. *Cell Mol Life Sci* **2017,** *74*, 3293–3303.
15. Flack, C. E.; Parkinson, J. S., A zipped-helix cap potentiates HAMP domain control of chemoreceptor signaling. *Proc Natl Acad Sci USA* **2018,** *115*, E3519–E3528.
16. Nishiyama, S.; Suzuki, D.; Itoh, Y.; Suzuki, K.; Tajima, H.; Hyakutake, A.; Homma, M.; Butler-Wu, S. M.; Camilli, A.; Kawagishi, I., Mlp24 (McpX) of *Vibrio cholerae* implicated in pathogenicity functions as a chemoreceptor for multiple amino acids. *Infect Immun* **2012,** *80*, 3170–3178.
17. Choi, Y.; Kim, S.; Hwang, H.; Kim, K. P.; Kang, D. H.; Ryu, S., Plasmid-encoded MCP is involved in virulence, motility, and biofilm formation of *Cronobacter sakazakii* ATCC 29544. *Infect Immun* **2015,** *83*, 197–204.
18. McLaughlin, H. P.; Caly, D. L.; McCarthy, Y.; Ryan, R. P.; Dow, J. M., An orphan chemotaxis sensor regulates virulence and antibiotic tolerance in the human pathogen *Pseudomonas aeruginosa*. *PLoS One* **2012,** *7*, e42205.
19. Yu, X.; Lund, S. P.; Scott, R. A.; Greenwald, J. W.; Records, A. H.; Nettleton, D.; Lindow, S. E.; Gross, D. C.; Beattie, G. A., Transcriptional responses of *Pseudomonas syringae* to growth in epiphytic versus apoplastic

leaf sites. *Proc Natl Acad Sci USA* **2013,** *110*, E425–434.
20. Matilla, M. A.; Krell, T., The effect of bacterial chemotaxis on host infection and pathogenicity. *FEMS Microbiol Rev* **2018,** *42*.
21. Ali, M.; Sun, Y.; Xie, L.; Yu, H.; Bashir, A.; Li, L., The pathogenicity of *Pseudomonas syringae* MB03 against *Caenorhabditis elegans* and the transcriptional response of nematicidal genes upon different nutritional conditions. *Front Microbiol* **2016,** *7*, 805.
22. Bashir, A.; Sun, Y.; Yu, X.; Sun, X.; Li, L., Nematicidal effects of 2-methyl-aconitate isomerase from the phytopathogen *Pseudomonas syringae* MB03 on the model nematode *Caenorhabditis elegans*. *J Invertebr Pathol* **2021,** *185*, 107669.
23. Ali, M.; Gu, T.; Yu, X.; Bashir, A.; Wang, Z.; Sun, X.; Ashraf, N. M.; Li, L., Identification of the genes of the plant pathogen *Pseudomonas syringae* MB03 required for the nematicidal activity against *Caenorhabditis elegans* through an integrated approach. *Front Microbiol* **2022,** *13*, 826962.
24. Kaletta, T.; Hengartner, M. O., Finding function in novel targets: *C. elegans* as a model organism. *Nat Rev Drug Discov* **2006,** *5*, 387–398.
25. Li, Q.; Yan, Q.; Chen, J.; He, Y.; Wang, J.; Zhang, H.; Yu, Z.; Li, L., Molecular characterization of an ice nucleation protein variant (InaQ) from *Pseudomonas syringae* and the analysis of its transmembrane transport activity in *Escherichia coli*. *Int J Biol Sci* **2012,** *8*, 1097–1108.
26. Sambrook, J.; Russell, D. W., Molecular cloning: a laboratory manual, 3rd ed. Cold Spring Harbor Laboratory Press, Cold Spring Harbor, N.Y. **2001**.
27. Porta-de-la-Riva, M.; Fontrodona, L.; Villanueva, A.; Cerón, J., Basic *Caenorhabditis elegans* methods: Synchronization and observation. *J Vis Exp* **2012**, *64*, e4019.
28. Bradford, M. M., A rapid and sensitive method for the quantitation of microgram quantities of protein utilizing the principle of protein-dye binding. *Anal Biochem* **1976,** *72*, 248–254.
29. Griffitts, J. S.; Whitacre, J. L.; Stevens, D. E.; Aroian, R. V., Bt toxin resistance from loss of a putative carbohydrate-modifying enzyme. *Science* **2001,** *293*, 860–864.
30. Manan, A.; Bazai, Z. A.; Fan, J.; Yu, H.; Li, L., The Nif3-family protein YqfO03 from *Pseudomonas syringae* MB03 has multiple nematicidal activities against *Caenorhabditis elegans* and *Meloidogyne incognita*. *Int J Mol Sci* **2018,** *19*, 3915
31. Paiano, A.; Margiotta, A.; De Luca, M.; Bucci, C., Yeast two-hybrid assay to identify interacting proteins. *Curr Protoc Protein Sci* **2019,** *95*, e70.
32. Green, M. R.; Sambrook, J., Total RNA extraction from *Caenorhabditis elegans*. *Cold Spring Harb Protoc* **2020,** *2020*, 101683.
33. Gibson, D. G.; Young, L.; Chuang, R. Y.; Venter, J. C.; Hutchison, C. A., 3rd; Smith, H. O., Enzymatic assembly of DNA molecules up to several hundred kilobases. *Nat Methods* **2009,** *6*, 343–345.
34. Zhu, J.; Cai, X. Q.; Harris, T. L.; Gooyit, M.; Wood, M.; Lardy, M.; Janda, K. D., Disarming *Pseudomonas aeruginosa* virulence factor LasB by leveraging a *Caenorhabditis elegans* infection model. *Chem Biol* **2015,** *22*, 483–491.
35. Conte Jr, D.; MacNeil, L. T.; Walhout, A. J.; Mello, C. C., RNA interference in *Caenorhabditis elegans*. *Curr Protoc Mol Biol* **2015,** *109*, 26.3.1–26.3.30.
36. Livak, K. J.; Schmittgen, T. D., Analysis of relative gene expression data using real-time quantitative PCR and the $2^{-\Delta\Delta CT}$ method. *Methods* **2001,** *25*, 402–408.
37. Qin, N.; Xu, D.; Li, J.; Deng, X. W., COP9 signalosome: Discovery, conservation, activity, and function. *J Integr Plant Biol* **2020,** *62*, 90–103.
38. Pintard, L.; Kurz, T.; Glaser, S.; Willis, J. H.; Peter, M.; Bowerman, B., Neddylation and deneddylation of CUL-3 is required to target MEI-1/Katanin for degradation at the meiosis-to-mitosis transition in *C. elegans*. *Curr Biol* **2003,** *13*, 911–921.
39. Inoue, H.; Hisamoto, N.; An, J. H.; Oliveira, R. P.; Nishida, E.; Blackwell, T. K.; Matsumoto, K., The *C. elegans* p38 MAPK pathway regulates nuclear localization of the transcription factor SKN-1 in oxidative stress response. *Genes Dev* **2005,** *19*, 2278–2283.
40. Broday, L.; Hauser, C. A.; Kolotuev, I.; Ronai, Z., Muscle-epidermis interactions affect exoskeleton patterning in *Caenorhabditis elegans*. *Dev Dyn* **2007,** *236*, 3129–3136.
41. Gerke, P.; Keshet, A.; Mertenskötter, A.; Paul, R. J., The JNK-like MAPK KGB-1 of *Caenorhabditis elegans* promotes reproduction, lifespan, and gene expressions for protein biosynthesis and germline homeostasis but interferes with hyperosmotic stress tolerance. *Cell Physiol Biochem* **2014,** *34*, 1951–1973.

42. Gieseler, K.; Qadota, H.; Benian, G., Development, structure, and maintenance of *C. elegans* body wall muscle. *WormBook* **2018,** *2017*.
43. Smith, P.; Leung-Chiu, W. M.; Montgomery, R.; Orsborn, A.; Kuznicki, K.; Gressman-Coberly, E.; Mutapcic, L.; Bennett, K., The GLH proteins, *Caenorhabditis elegans* P granule components, associate with CSN-5 and KGB-1, proteins necessary for fertility, and with ZYX-1, a predicted cytoskeletal protein. *Dev Biol* **2002,** *251*, 333–347.
44. Yoon, D. S.; Cha, D. S.; Choi, Y.; Lee, J. W.; Lee, M. H., MPK-1/ERK is required for the full activity of resveratrol in extended lifespan and reproduction. *Aging Cell* **2019,** *18*, e12867.
45. Miller, R. K.; Qadota, H.; Stark, T. J.; Mercer, K. B.; Wortham, T. S.; Anyanful, A.; Benian, G. M., CSN-5, a component of the COP9 signalosome complex, regulates the levels of UNC-96 and UNC-98, two components of M-lines in *Caenorhabditis elegans* muscle. *Mol Biol Cell* **2015,** *20*, 3608–3616.
46. Geng, C.; Liu, Y.; Li, M.; Tang, Z.; Muhammad, S.; Zheng, J.; Wan, D.; Peng, D.; Ruan, L.; Sun, M., Dissimilar crystal proteins Cry5Ca1 and Cry5Da1 synergistically act against *Meloidogyne incognita* and delay Cry5Ba-based nematode resistance. *Appl Environ Microbiol* **2017,** *83*, e03505–e03516.
47. Kim, T.; Hofmann, K.; von Arnim, A. G.; Chamovitz, D. A., PCI complexes: pretty complex interactions in diverse signaling pathways. *Trends Plant Sci* **2001,** *6*, 379–386.
48. Zhang, S. N.; Pei, D. S.; Zheng, J. N., The COP9 signalosome subunit 6 (CSN6): a potential oncogene. *Cell Div* **2013,** *8*, 14.
49. Braus, G. H.; Irniger, S.; Bayram, Ö., Fungal development and the COP9 signalosome. *Curr Opin Microbiol* **2010,** *13*, 672–676.
50. Sandhu, A.; Badal, D.; Sheokand, R.; Tyagi, S.; Singh, V., Specific collagens maintain the cuticle permeability barrier in *Caenorhabditis elegans*. *Genetics* **2021,** *217*, iyaa047.